

Postdeposition annealing of ITO films produced by r.f. magnetron sputtering.

M. Cruz-Jáuregui¹, J. M. Siqueiros^{1,2}, R. Machorro² and S. Wang².

¹Centro de Investigación Científica y de Educación Superior de Ensenada., A. Postal 2681, 22800 Ensenada B.C., México. Programa de posgrado.

²Instituto de Física, UNAM., Laboratorio de Ensenada, A. Postal 2681, 22800 Ensenada B.C., México.

Indium tin oxide (ITO) films of 1000 Å thick were deposited on glass substrates by r.f. magnetron sputtering. The effect of post-deposition heat treatment on electrical and optical properties of ITO films was investigated. The annealing experiments were carried out in an air atmosphere, at temperatures from 150°C to 550°C, for one hour. The results show that resistivity increases with temperature, from $2.5 \times 10^{-4} \Omega \cdot \text{cm.}$, until it reaches a maximum where it stays constant (temperatures between 200°C and 250°C), and then starts decreasing approaching the initial value. Such behavior is explained through grain boundary measurements performed in a STM system. Transmittance spectra, obtained with a spectrophotometer, show an increase in band gap energy for post-annealing temperatures higher than 300°C which may be produced by an increase in carrier density. Film thickness was determined with a quartz microbalance and a profilometer; AES and EDS were used for chemical analysis and the four point probe technique was employed for resistivity measurements.

keywords: ITO, transparent conductors.

PACS numbers: 78.66.-, 81.15.Cd, 81.40.-z.

INTRODUCTION.

The relevant feature that makes ITO ($\text{In}_2\text{O}_3:\text{SnO}_2$) technologically important is the coexistence of otherwise mutually excluding properties, that is, good electrical conductivity and high transparency to the visible spectrum; additionally, it is a good infrared reflector. That is why ITO is used in a great variety of electronic and optoelectronic applications such as transparent electrodes [1] photovoltaic devices [2], display devices [1], antireflection coatings [3], etc.

ITO films have been deposited by different techniques such as spray pyrolysis [4,5], thermal and electron-beam evaporation [4,6,7], chemical vapor deposition [4], sputtering (d.c., r.f. and magnetron) [4,8-10] and pulsed laser ablation [11]. R.f. magnetron sputtering has proven to be (together with laser ablation) one of the best techniques for preparing ITO films, mainly due to its high deposition rates, deposition over large areas, good quality of films, and because it very closely preserves the stoichiometry of the alloy material used as a target.

The properties of ITO films grown by r.f. magnetron sputtering depend strongly on the deposition parameters such as the base pressure of the chamber, work pressure of the sputtering gas, target to substrate distance, deposition rate, temperature of the substrate, and post-deposition heat treatment [4,6,12-16].

In this work, we report the characterization and effect of post-deposition annealing in air, on the electrical and optical properties of ITO films deposited by r.f. magnetron sputtering.

EXPERIMENTAL PROCEDURE.

ITO films were deposited on glass substrates at room temperature by r.f. magnetron sputtering. The sputtering target was a 2" disc of $\text{In}_2\text{O}_3:9\% \text{mol}:\text{SnO}_2$ from Target Materials Inc. with a 99.99% purity and was fabricated by mixing and pressing In_2O_3 and SnO_2 powders in the appropriate relation. The target-substrate distance was 5cm. and the substrates were placed parallel to the target surface. The sputtering chamber was evacuated to a residual vacuum of 3.2×10^{-6} Torr. The sputtering gas was argon, at work pressures of 1.5 Torr and 2 Torr. The forward power (at 13.56 MHz) were 20 and 22 watts. The reflected power was around 1.5 watts for both cases.

To remove possible contaminants and the surface oxide layer formed on the target during exposure to air and avoid its deposition on the substrate, a shutter was interposed between the target and the substrate for five minutes before letting the sputtered material reach the substrate. A deposition rate of 1 Å/seg was fixed by a quartz microbalance controller.

Film thickness was measured with a stylus profilometer (Dektak-3 of Veeco Instruments Inc.).

Auger electron spectroscopy (AES) and energy dispersion spectroscopy (EDS) were used to determine the chemical composition of target and films. The system used in AES was a PHI-595 by PERKIN-ELMER. The EDS measurements were made in a JEOL JSM-5300 system.

The annealing treatment was performed in air for one hour at temperatures in the 150-550 °C interval.

The film resistivity was obtained with a four point probe measuring device made in our laboratory. A 224 current

supply and a 125A multimeter, both by Keithley, were used. The separation between probes is 0.4mm.

The photometric spectra were obtained with a spectrophotometer designed and made in our own laboratory. Its wavelength range is 300 nm to 800 nm.

The surface topology and grain size were determined by scanning tunneling microscopy (STM), (NanoScope 1 by Digital Instruments).

Finally, Hall effect measurements were carried in the van der Pauw configuration.

RESULTS AND DISCUSSION.

Figure 1 shows the graph produced by the profilometer as we scanned along the substrate-film step. We can see that the film thickness is not uniform along the whole sample surface the reason being that the sample mass distribution seems to image the plasma distribution generated for the deposition process. Nevertheless, we found a zone of 4.5 cm. in diameter where the films were uniform with a thickness of $1000 \pm 100 \text{ \AA}$. Film thickness determination of ITO films is quite important because some of their more relevant properties, namely resistance, depend strongly on it.

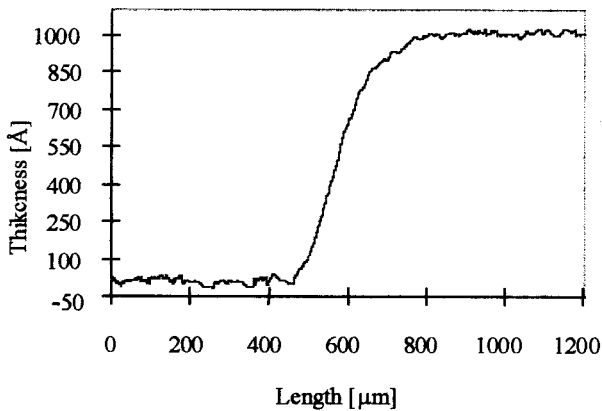


Fig 1.- Profile of an ITO deposited film , produced by the profilometer.

In ITO films, SnO_2 (Sn valence 4) is introduced into a In_2O_3 (In valence 3) matrix to supply an additional electron per atom as Sn^{4+} ions substitute the In^{3+} in the cation sublattice. As a result, the $\text{In}_2\text{O}_3:\text{SnO}_2$ thus produced becomes a highly n-doped semiconductor. It has been determined that a 10% of SnO_2 gives the optimum relative concentration [8] for the best transmittance-reflectance characteristics and lowest resistivity.

One of the principal features of the sputtering deposition technique is the conservation of the stoichiometry of the target in the films. AES and EDS quantification was used to verify stoichiometry conservation and therefore the correct In-Sn relation in the target and films. Before AES

measurements, the samples were cleaned with argon ions. Because of the requirements of the technique, 3 μm thick films had to be used for EDS to obtain reliable measurements. The results are shown in table 1:

Table 1. AES and EDS measurements of ITO films and target.

	in the target		in the films:		
	AES	EDS	AES	EDS	
In	86 %	87 %	In	89 %	91 %
Sn	14 %	13 %	Sn	11 %	9 %

As we can see from our own measurements the Sn content in the target comes out higher than that specified by the manufacturer. Apparently, 2% of Sn is lost in the sputtering process and, as a consequence the Sn content in the films is closer to the ideal 10%.

The ITO film resistivity was measured before and after heat treatment. Figure 2 shows the values of the ITO film resistivity as a function of annealing temperature. We observed that the resistivity increased from $2.5 \times 10^{-4} \Omega\text{-cm}$ to a maximum of $11.7 \times 10^{-4} \Omega\text{-cm}$ where it reaches a plateau and then decreases to $4.9 \times 10^{-4} \Omega\text{-cm}$. The first value of resistivity corresponds to the films without the annealing treatment; the second one is associated to a temperature range of 200 °C to 250 °C, and the last one is for the maximum annealing temperature (550 °C).

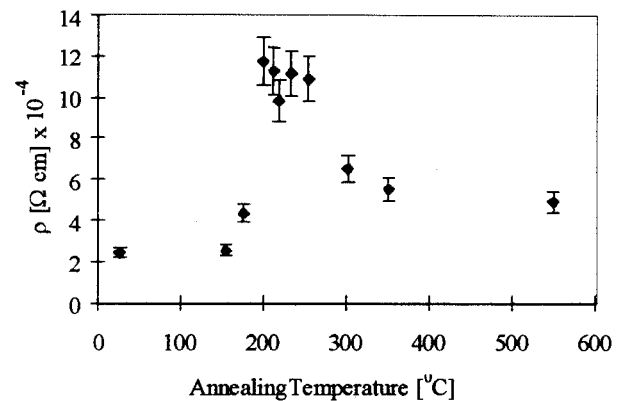


Fig. 2 Resistivity of the ITO films as a function of annealing temperature.

This behavior is different from most of the previously reported results where a decrease in resistivity with annealing temperature [13,14,16] or a decrease and then an increase [15] is usually observed.

We can explain our resistivity curves based on carrier scattering by grain boundaries supported by STM measurements. Figure 3 shows STM images of two different zones of ITO films without treatment (Fig. 3.a), annealed at 200°C-250°C (Fig. 3.b), and annealed at 550°C (Fig. 3.c). Films as deposited have the largest grain size which implies that dispersion by grain boundaries will

be smaller. For temperatures in the 200°C to 250°C range, grains are the smallest with several zones where grains could not be resolved. Here we expect the resistivity increment to be due to an increase of the scattering by grain boundaries.

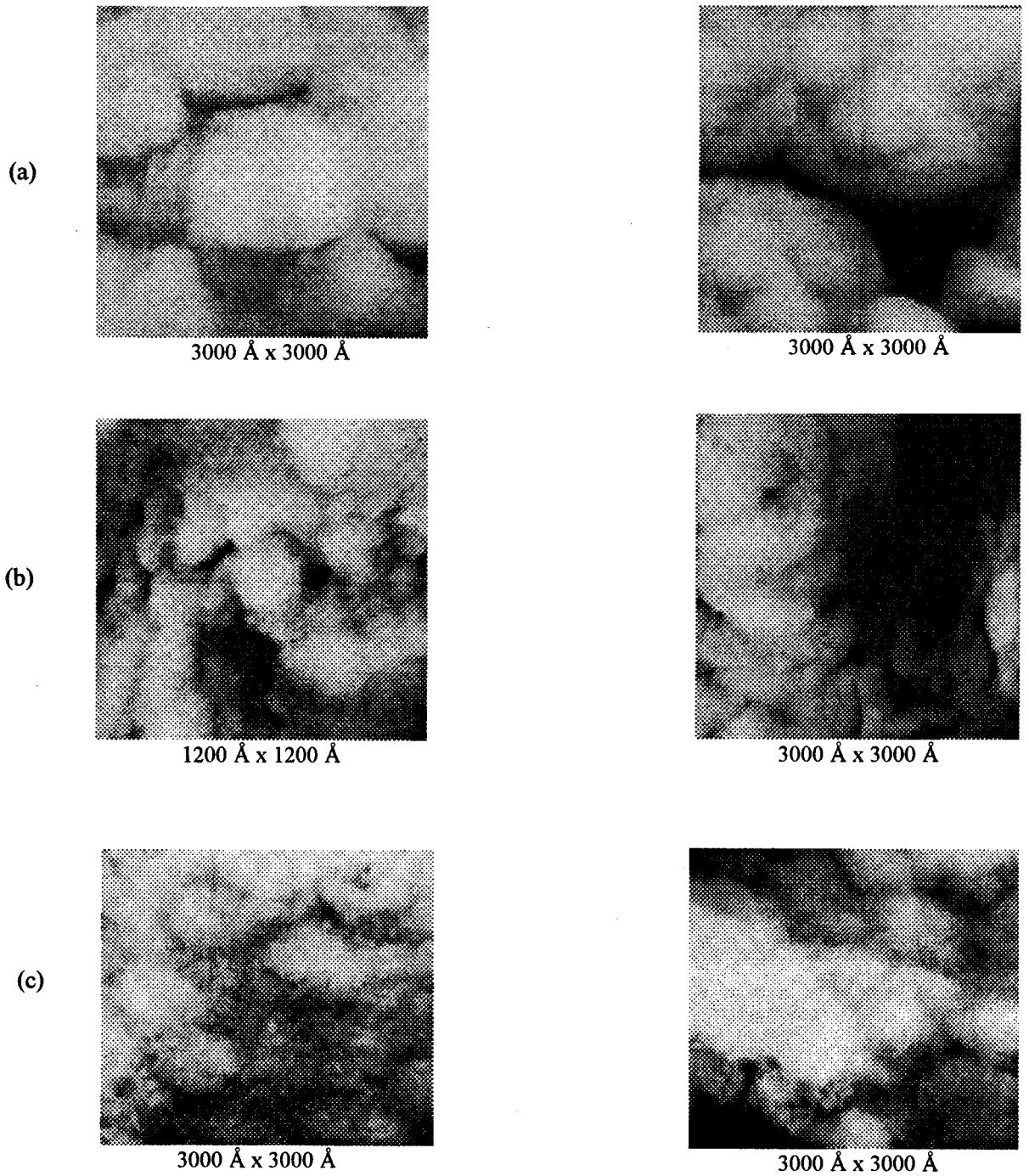


Fig.3. STM images of the ITO films, in two different regions a) without heat treatment, b) annealed at 200°C - 250°C, and c) annealed at 550°C.

Figure 4 shows transmittance curves of post-annealed films. If we compare this result with those of films before annealing, we find a maximum difference of 3%.

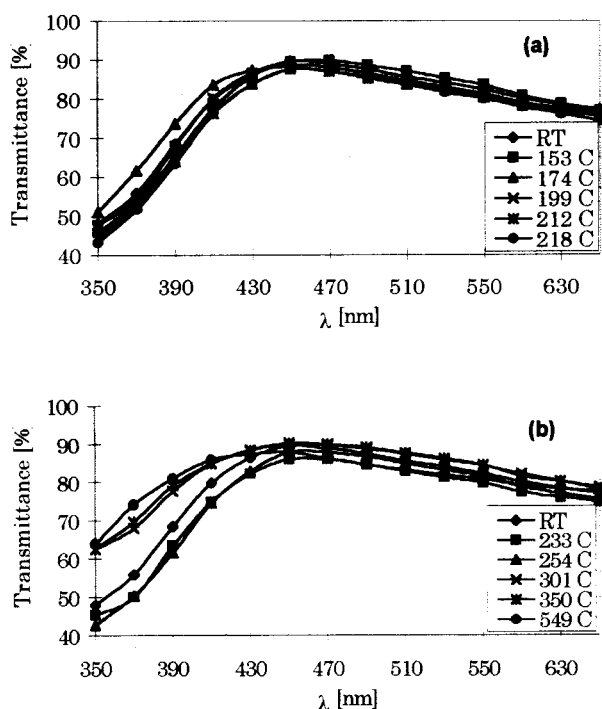


Fig. 4.- Transmission spectra of ITO films annealed at a)150 °C-218 °C and, b)233 °C-549 °C.

The only, and obvious change in spectral behavior is the shift of the transmittance curve toward lower wavelength values for ITO films annealed at temperatures higher than 300°C. This is an indication of an enhancement of the energy gap, due to the Burstein-Moss effect [17] given by:

$$\Delta E_{BM} = \frac{h}{2m^*} \left(\frac{3n}{\pi} \right)^{\frac{2}{3}} \quad (1)$$

where n is the carrier density and m^* is the electron effective mass equal to $0.55m_e$ [18]. A maximum increment of 0.22eV in the energy gap is observed as a consequence of the heat treatment, this is shown in table II.

Table II. ΔE_{BM} calculated for ITO films as deposited and annealed at 550 °C using our experimental values in Eq. 1.

Annealing Temperature [°C]	Density Carrier [1/cm ³]	Burstein-Moss Shift [eV]
As deposited	6.58×10^{20}	0.50
550	1.15×10^{21}	0.72

CONCLUSIONS.

ITO films of $1000 \pm 100 \text{ \AA}$, with good thickness uniformity in a region of 4.5 cm. in diameter were deposited by a r.f. magnetron sputtering technique.

For annealing temperatures higher than 300 °C there is an increase in the energy band gap that is explained by an increase in the carrier density.

The behavior of the resistivity for post-deposition annealed ITO films can be explained in terms of the changes in grain size. Larger grains and uniformity means less dispersion at grain boundaries therefore, lower resistivity.

ACKNOWLEDGMENTS.

We would like to thank: J. Nieto, J. Valenzuela, G. Soto, and I. Gradilla for their technical assistance.

M. Cruz-Jáuregui thanks CONACYT for the financial support (scholarship No. 88686).

This work was partially supported by CONACYT. Proy. No. 4143E.

REFERENCES.

- [1] R. Latz, K. Michael and M. Scherer, *Jnp. J. Appl. Phys*, **30** (1991) L149.
- [2] A.C. Rastogi and S.T. Laskhmikumar, *Sol. Cell.*, **26** (1989) 323.
- [3] I. Hamberg, A. Hjortsberg and C.G. Granqvist, *Appl. Phys. Lett.*, **40** (1982) 362.
- [4] Z. M. Jarzebski, *Phys. Stat. Sol. (a)*, **13** (1982) 13-41.
- [5] Ph. Parent, et. al. *J. Electrochem. Soc.*, **139** (1992) 276-281.
- [6] F. M. Amanullah, K. J. Pratap, and V. Hari Babu. *Thin Solid Films*, **254** (1995) 28-32.
- [7] A. Hjortsberg, I. Hamberg, and C.G. Granqvist, *Thin Solid Films*, **90** (1982) 323.
- [8] Vossen. *RCA Review*, **32** (1971) 289-297.
- [9] S. Chaudhuri, J. Bhattacharyya, and A. K. Pal. *Thin Solid Films*, **148** (1987) 279-284.
- [10] Y. Shigesato, S. Takaki, and T. Haranoh. *Appl.Surf. Sci.*, **48/49** (1991) 269-275.
- [11] J. P. Zheng and H. S. Kwok. *Appl. Phys. Lett.*, **63** (1993) 1-3.
- [12] C. H. L. Weijtens and P. A. C. Van Loon. *Thin Solid Films*, **196** (1991) 1-10.
- [13] M. A. Martínez, J. Herrero, and M. T. Gutiérrez. *Solar Energy Materials and Solar Cells*, **26** (1992) 301-321.
- [14] Wen-Fa Wu and Bi-Shiou Chiou. *Appl. Surf. Sci.*, **68** (1993) 497-504.
- [15] M. Higuchi, A. Macarico, and R. Martins. *Jpn. J. Appl. Phys.*, **33** (1994) 302-306.
- [16] L1-Jian Meng, A. Macarico and R. Martins. *Vacuum*, **46** (1995) 673-680.
- [17] E. Burstein. *Phys. Rev.*, **93** (1954) 632.
- [18] R.L Weiher *Phys. Rev.*, **33** (1962) 2834.